The Effect of Salt Weathering and Water Absorption on the Ultrasonic Pulse Velocities of Highly Porous Limestone

Mohammad Ali Khodabandeh[1*], Nikoletta Rozgonyi-Boissinot[1]

[1] Department of Engineering Geology and Geotechnics, Faculty of Civil Engineering, Budapest University of Technology and Economics, H-1111 Budapest, Műegyetem rkp. 3., Hungary
[*] Corresponding author, e-mail: mohammad.khodabandeh@emk.bme.hu

Abstract

One of the major causes of building stone deterioration is salt crystallization. In this study, changes of ultrasonic pulse velocities of highly porous limestone (obtained from the Sóskút quarry, Hungary) during capillary water absorption, water saturation and during salt crystallization tests were investigated. Capillary water absorption and water saturation tests were carried out according to EN 1925 and EN 13755. In salt crystallization test, the samples were submerged in salt solutions of 14 % Na_2SO_4 (according to EN 12370) and 5% NaCl solution. The weight changes and ultrasonic pulse velocities of samples were measured after each salt crystallization cycle. During capillary water absorption and water saturation tests, the P and S waves velocities of samples increased as the water content increased. Salt crystallization occurred at the beginning increase of P wave velocity due to the accumulation of salts in the pores. Propagation of P wave was decreased with additional salt crystallization cycles due to the opening of micro-cracks in the samples. The trend of S wave velocity was different from the trend of P wave velocity because it was increasing from non-weathered samples to 50 cycles of salt crystallization. According to the results of the elastic waves measurements and the mass changes, sodium sulphate was found to be more destructive in the weathering of limestone than sodium chloride.

Keywords

salt crystallization, sodium sulphate, sodium chloride, ultrasonic wave velocity, porous limestone

1 Introduction

The most important issues and the most serious phenomena that contribute to the degradation of both cultural heritages and modern buildings are water absorption and salt crystallization [1]. Porosity, pore size distribution and environmental factors influence how moisture is distributed inside rocks. Low porosity stones with a large number of small pores (<1 μm) are less vulnerable to decay than high porosity rocks with a larger average pore radius if their pore network has high tortuosity and low connectivity. Low connectivity decreases water flow capability [2]. Salt decay occurs with the simultaneous presence of soluble salts and water in a porous material as a result of the crystallization/dissolution cycle [3]. Water is a significant factor in the weathering and chemical reactions of building materials and controls the transport, crystallization, and hydration of salts [4]. Water is transported by open pores in porous building stones, mostly due to capillary water absorption. The amount of water that can enter the pores and micro cracks of the stones is determined by the capillary water absorption test. Stones with high porosity and high capillary water absorption coefficient are considered to have a significant damage potential [5].

Çelik and Kaçmaz [6] carried out capillary water absorption test for three types of stone including two tuff stones and andesite in normal and salty water conditions (14w% NaCl). The results showed that capillary water absorption of salty water was higher than that of clean water. Sengun et al. [7] investigated capillary water absorption coefficient of 118 different natural stone types (12 igneous, 29 metamorphic, 77 sedimentary). The results showed a linear relationship between capillary water absorption coefficient and density or porosity. An inverse relationship was observed between capillary water absorption coefficient and uniaxial compressive strength or ultrasonic wave velocity. Çelik [8] investigated the increasing of P wave velocity of travertine after water saturation and freeze-thaw process.

Barbera et al. [9] investigated changes in longitudinal wave velocity of limestone (porosity ca. 20 V%) subjected

to water absorption and salt crystallization tests (14 w% $Na_2SO_4.10H_2O$). The results showed a reduction in P wave velocity after 8 salt cycles due to the formation of macro- and micro-fractures within the pore structure caused by the growth of salt crystals. The most porous samples had the highest hydric parameters (capillary absorption coefficient and saturation index) and the highest mass losses due to salt crystallization.

Rodriguez-Navarro and Doehne [10] investigated the effects of salt crystallization on oolitic limestone with sodium sulphate solution (16.13 w%) and sodium chloride solution (26.41 w%). Stones were placed in a salt solution, and crystallization occurred in the upper exposed stone areas after the capillary rise. The results showed that evaporation rate plays an important role in the rate of damage and the growth of both thenardite and mirabilite crystals was responsible for the damage, depending on the relative humidity (RH). The damage was often higher at low humidity and temperatures leading to thenardite crystallization. At low RH conditions, sodium chloride can also generate more damage, but the amount of damage caused by halite growth is much less than the amount of damage caused by sodium sulphate. The results showed that the weathering properties of sodium chloride and sodium sulphate differ due to differences in solution physical properties (e.g., surface tension and vapor pressure) and crystallization patterns.

Angeli et al. [11] stated that the damage caused by salt crystallization is according to three stages. At first, due to the addition of salts to the pores and filling pore space of the samples, the weight of samples increases, and consequently, their porosity reduces. After filling the pores, the weight of samples decreases slightly (stage 2). Stage 3 starts as salt uptake become negligible in comparison to material loss. During stage 3, the pores are expected to be filled with salt. Supersaturation in relation to mirabilite happened at each cycle. The salts crystallized and caused damages to the cracks and pores. As a result, the more pre-existing cracks and pores in the rock caused more damages and lower P wave velocity [11].

Methods based on elastic wave analyses are widely used in geotechnical engineering. Both laboratory and field studies can benefit from these non-destructive techniques. The elastic wave velocities of rocks are influenced by a variety of factors including density, mineralogy, grain size, porosity and pore size as well as pressure, temperature, water content [12, 13] and weathering due to the changes in microstructure [14].

In order to evaluate the elastic properties of stones on a non-destructive way, determining compressional or longitudinal wave (P wave) and transversal or shear wave (S wave) is essential [15]. Uyanık et al. [16] investigated the P and S waves velocities of three types of stone including limestone, sandstone and siltstone. The correlation coefficients were measured between some parameters including densities, void ratio, and porosity with ultrasonic wave velocities and were higher than 67%. The results showed that when the physical (densities, porosity, void ratio) and mechanical properties (UCS) of rocks were determined only based on P wave velocity, there were more errors than when they were based on both P and S waves velocities.

In the present study, capillary water absorption and water saturation tests were carried out to investigate the capillary water uptake coefficient, saturation degree and ultrasonic pulse velocities of non-weathered stones in a short and long period of time. Changes in ultrasonic pulse velocities (P and S waves) of limestone exposed to salt solutions of 14 w% Na_2SO_4 (based on EN 12370 [17]) and 5 w% NaCl solution were investigated. Ultrasonic wave velocities of samples were measured by two devices including Pundit (Portable Ultrasonic Non-destructive Digital Indicating Tester) and Geotron (Consonic C2-GS Geotron Elektronik). P wave velocities of samples were determined before salt crystallization and after each salt cycle by Pundit equipment. P and S waves velocities of samples were measured after 15 and 50 salt cycles by Geotron equipment.

2 Materials and methods

Fourteen cylindrical limestone specimens were sampled from the Sóskút quarry (in Hungary). The investigated stone was Miocene, coarse grained and high porous oolithic limestone with macropores between 1 and 12 mm and with maximum grain size of 5 mm. Characteristic feature of this stone is small density (1.504–1.733 g/cm³), high porosity (22–31 V%), large pores (up to 12 mm) and low p wave velocity (2.33–2.59 km/s) (Table 1). The physical properties of the limestone from the Sóskút quarry vary depending on the lithology, however, the limestone has high porosity and low strength. In quarries, Miocene oolitic limestone has a yellowish-white color and its most common mineral is Calcite ($CaCO_3$). Also, it contains minor amounts of quartz and feldspars, which are mostly observed in ooid cores. There were some primary carbonate particles including well-to-moderately rounded ooids and micro-oncoids with diameters of 0.2–1.0 mm and also other components such

Table 1 Physical properties of the samples

Salt solution	Sample code	Density (air dry) gr/cm³	P wave velocity of fresh samples (km/s)	Porosity (V%)
no (Group A)	1	1.559	2.66	29.61
	2	1.479	2.33	30.89
	3	1.736	3.25	22.24
	4	1.538	2.54	28.24
14 w% Na₂SO₄·10H₂O (Group B)	SC15-1	1.525	2.43	-
	SC15-2	1.504	2.41	-
	SC50-1	1.541	2.59	-
	SC50-2	1.550	2.58	-
	SC50-3	1.570	2.62	-
5 w% NaCl (Group C)	CL15-1	1.489	2.41	-
	CL15-2	1.528	2.46	-
	CL50-1	1.538	2.49	-
	CL50-2	1.518	2.49	-
	CL50-3	1.509	2.47	-

Fig. 1 Photos of samples before salt crystallization a) sample SC50-2 and b) sample SC50-3

as red algae fragments, gastropods, bivalves and foraminifera. The majority of pores are intergranularly linked, resulting in a high effective porosity (up to 22 percent). Intergranular pores are typically 1–12 mm in diameter, however, intragranular pores are frequently smaller [18]. Regarding the texture of the stone, the size of ooids and the number of other particles is variable, but the most common types are ooid grainstone and bioclastic ooid grainstone [18]. The oolitic varieties are also used extensively in Budapest's building [19] which are severely decayed and in many cases severely weathered. The pore structure and the amount of fossils determine the stone's frost resistance, which ranging from non-frost-resistant to frost-resistant [20]. The Miocene oolitic limestone in Budapest is texturally comparable to several other oolitic construction limestones, such as Italian oolitic limestone (latomia quarry in Maddalena peninsula) [21], British Great Oolite (Monks Park limestone) [22] or the French Jaumont limestone [23], however it has higher porosity, lighter color, and lower strength [18].

Specimens were classified into three groups (A, B, C). In each group, stone samples with different parameters were placed. The height of samples was between 29 mm and 38 mm and the diameter of samples was 37 mm. Macroscope photos of samples before salt crystallization are shown in Fig. 1. Two samples were different from the other samples: sample 3 had higher density (1.733 g/cm³) than other samples and on the sample surface of the SC50-3 were some cracks at the beginning of the experiment (Fig. 1(b)).
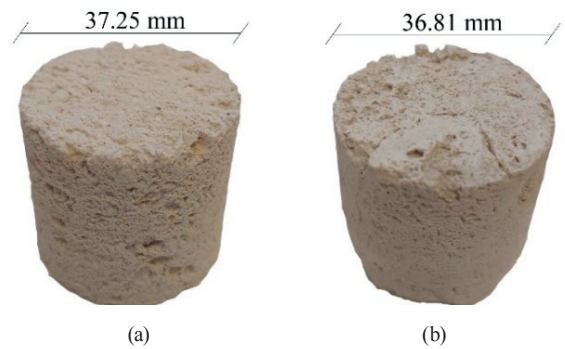
The samples of group A were kept without salt crystallization as a reference. Capillary water absorption tests (EN 1925 [24]) were carried out on these samples. At first, the sample dried into the oven at 105 °C for 48 hours. Then, the sample's base was placed in water to a depth of 5 mm. Different time ranges (1, 2, 3, 4, 5, 6, 7, 8, 9, 10, 15, 30, 60, 90, 120, 180, 300 minutes) were used to measure capillarity and to estimate the amount of absorbed water as a function of time. P wave velocity was measured after weighing the samples in each certain interval. Capillary water absorption coefficient was calculated based on two ways. At first, the curves of capillary water absorption (kg/m²) versus time (s0.5) were plotted based on Eq. (1). The slope of the curves and the maximum amounts of the curves were determined as the capillary water absorption coefficient based on the standard EN 1925 [24] and Çelik [6], respectively.

$$CWA = \frac{m_i - m_d}{A\sqrt{t}} \tag{1}$$

CWA = Capillary water absorption coefficient, (kg/m². s^{0.5})
m_i = Successive mass of the specimen during the test (kg),
m_d = dry mass of sample (kg),
A = Area of the bottom side of the specimen immersed in water (m²),
t = Time from beginning of the test until the time at which the successive mass mi was measured (s).

Water saturation under atmospherically pressure tests for non-weathered samples (group A) was performed according to the standard procedure of EN 13755 [25]. Dried samples were submerged in water at first up to half of the height of the samples. Every minute starting from 1 until 10 minutes, after 15 and 30 minutes, the samples were weighed, and the ultrasonic pulse velocity of samples was measured. After 1 hour, water was added until the level of the water reached three-quarter of the height of the

samples and the process of measuring weight and ultrasonic pulse velocity was repeated. After 2 hours, water was added until the samples were completely immersed to a depth of 25 + 5 mm of water and the weight and ultrasonic pulse velocities of samples were measured. Finally, the samples were weighed every 24 ± 2 hours and ultrasonic pulse velocities of samples were determined each time. Degree of saturation (S_r) was defined in Eq. (2).

$$S_r = V_W / V_V \times 100 \qquad (2)$$

S_r = degree of saturation (%)
V_W = Volume of absorbed water in the sample (cm³)
V_V = Volume of open pores in the sample (cm³)

Salt crystallization tests were performed on the samples of group B and C. These samples were artificially weathered by complete immersion in a 14 w% sodium sulphate decahydrate (based on EN 12370 [17]) solution and a 5 w% sodium chloride solution, respectively. The test included series of 24-hour cycles and each salt crystallization cycle consisted of:

- Immersion phase: 2 hours of immersion in a 14 w% sodium sulphate decahydrate solution (Group B) or a 5 w% sodium chloride solution (Group C) in 20 °C.
- Drying phase: The samples were dried in a ventilated oven. In 10 hours, the temperature was gradually increased to 105 °C, and kept there for another 10 hours.
- Cooling phase: The samples were kept at room temperature (20 °C) for 2 hours. During this period, mass change and ultrasonic pulse velocity were measured and the damages on the surface of the stones were investigated by optical microscope.

15 salt crystallization cycles were performed on two samples and 50 salt crystallization cycles were applied on three samples of each group. After salt crystallization, the samples were not washed out in water. After each salt crystallization cycle, the ultrasonic wave velocities were determined using two devices (Pundit and Geotron). Pundit equipment consisted transducers with a frequency of 50 kHz for determining the p-wave transmission time. To cover the space between the transducers and the sample plasticine was used. In case of the Geotron equipment, the wave was generated by UP-SW transducers (frequency of 80 kHz) and a Consonic C2-GS ultrasonic generator manufactured by Geotron-Elektronik. Determination of P and S waves arrival with Geotron equipment was based on methodology considered by Rozgonyi-Boissinot et al. [26] In this study, all measurements were repeated five times.

3 Results

The changes of P wave velocity against dried density are presented in Fig. 2. The results show that with increasing density, although P wave velocity had some fluctuations, but the general trend of P wave velocity was increasing. The minimum amount of P wave velocity was 2.33 km/s, and the maximum amount was 3.25 km/s. Except for sample 3, which had the highest dried density and P wave velocity, the rest of the samples had a dried density between 1.48 gr/cm³ and 1.57 gr/cm³ and a P wave velocity between 2.33 km/s and 2.66 km/s.

The results of capillary water absorption tests for non-weathered samples (Group A) are represented in Fig. 3. The changes of water content (V%) versus the square root of time are presented in Fig. 3(a). The curves can be divided into two zones. The first zone represented water absorption, the capillary absorption increased linearly with the square root of the elapsed time. The second zone had a lower slope, the water level reached to the end of the sample and further absorption was much slower.

According to Fig. 3(a) two samples (sample 2 and 4) entered to the second phase faster (after 2 and 3 minutes) and two samples (samples 1 and 3) reached it after 10 minutes. With visual investigation in the laboratory, capillary uptake reached to the top of the samples in 120, 120, 360 and 900 seconds for samples number 4, 2, 1 and 3, respectively. Fig. 3(a) shows a similar form of the curve in the first phase for samples 2 and 4 and samples 1 and 3, respectively. It was attributed to difference in the physical parameters of stone including density, porosity, and size of pores. Samples 2 and 4 had lower density rather than samples 1 and 3.

The capillary water absorption coefficient was calculated based on two ways. The results are represented in Fig. 3(b). In the first way after Çelik [6], the maximum amount of capillary water absorption on the curves were 9.64, 7.91, 7.88 and 6.18 kg/m². s0.5 for samples 2, 1, 4 and 3, respectively.
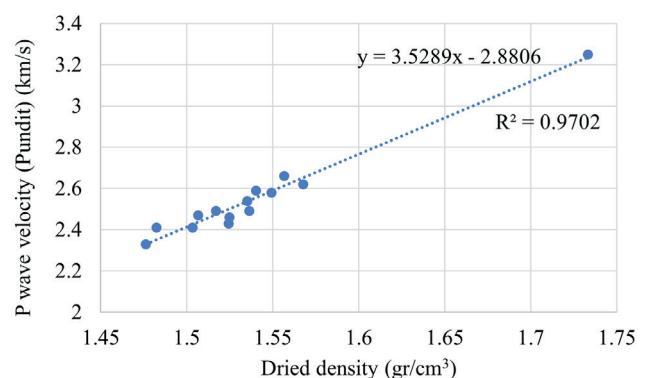

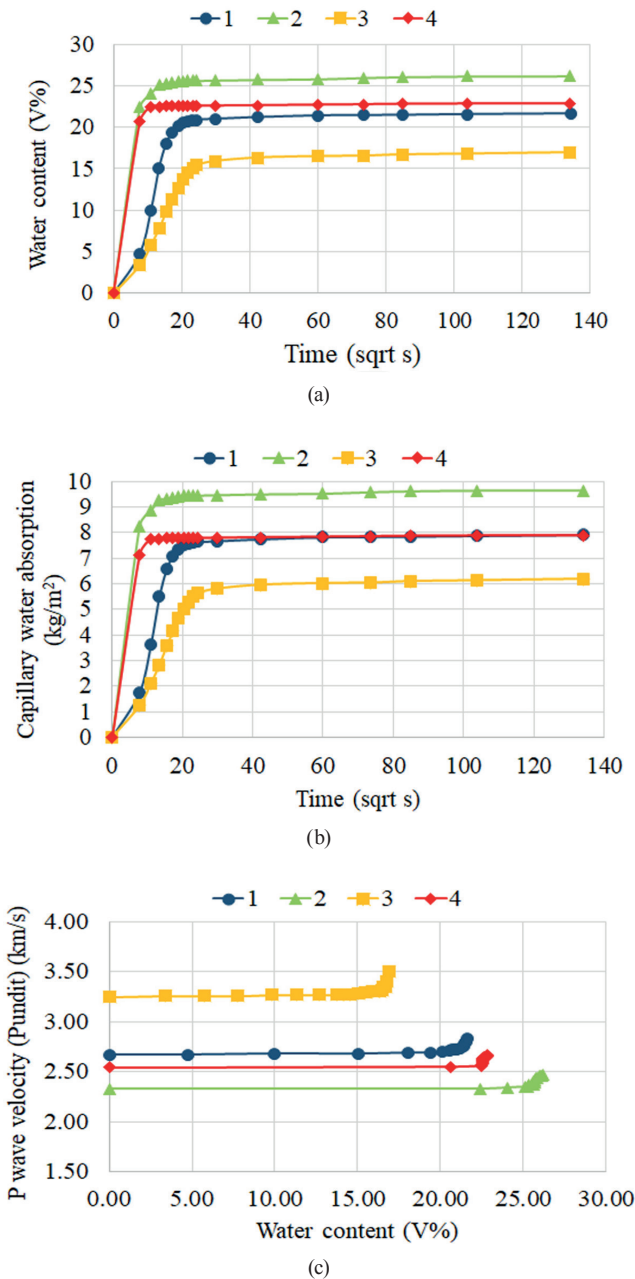**Fig. 2** P wave velocity change vs. dried density

(a)

(b)

(c)

Fig. 3 The results of capillary water test a) water content (V%) vs. time, b) capillary water absorption vs. time, c) P wave velocity vs. water content (V%)

Based on the second way (EN 1925 [24]), the slope of the curves was calculated as capillary water absorption coefficient. The results show that the highest amounts of capillary water absorption coefficient were 1.065 kg/m². s0.5 and 0.918 kg/m². s0.5 (samples 2 and 4) and the lowest amounts of capillary water absorption coefficient were 0.36 kg/m². s0.5 and 0.76 kg/m². s0.5 (sample 3 and 1).

The relationships between P wave velocities and water content (V%) are exhibited in Fig. 3(c). The trend of P wave velocity was different. The reason was the difference

in water absorption coefficient and consequently the difference in time to reach the saturation phase. However, P wave velocities were almost constant at the beginning and after reaching the saturation phase, the P wave velocity increased rapidly (Fig. 3(c)). The results of water saturation under atmospheric pressure tests for non-weathered samples are represented in Fig. 4.

The changes in water content (V%) against the square root of time were determined and are indicated in Fig. 4(a). Enlarged graph for water content (V%) versus square root of time in the first phase are shown in Fig 4(b). The results show two characteristic types of the curves. Samples 2 and 4 immediately reached the saturation phase but the others entered the saturation phase gradually. Sample 3 was the first to achieve its maximum saturation, while it took longer for other samples (Fig. 4(b)). Comparing Fig. 3 with Fig. 4 reveals that water uptake behavior of the stones was similar in case of both investigated water uptake tests. The order of reaching of the saturation phases (second part of the curves) was also the same.

The ultrasonic wave velocities corresponding to different water contents (V%) were measured (Fig. 5). Based on Geotron measurement, Fig. 5(a) represents how the P wave
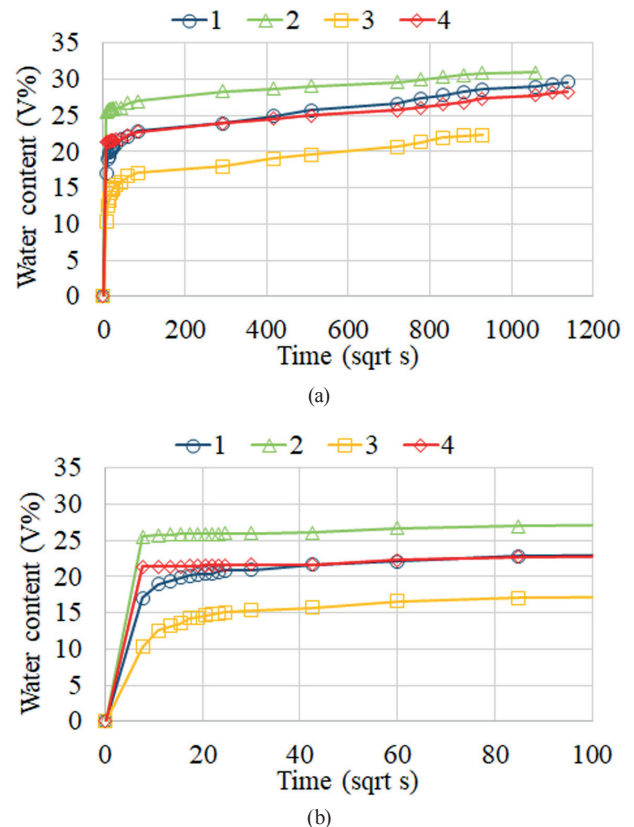

(a)

(b)

Fig. 4 The results of water saturation test a) water content (V%) vs. time, b) enlarged graph of water content (V%) vs. time
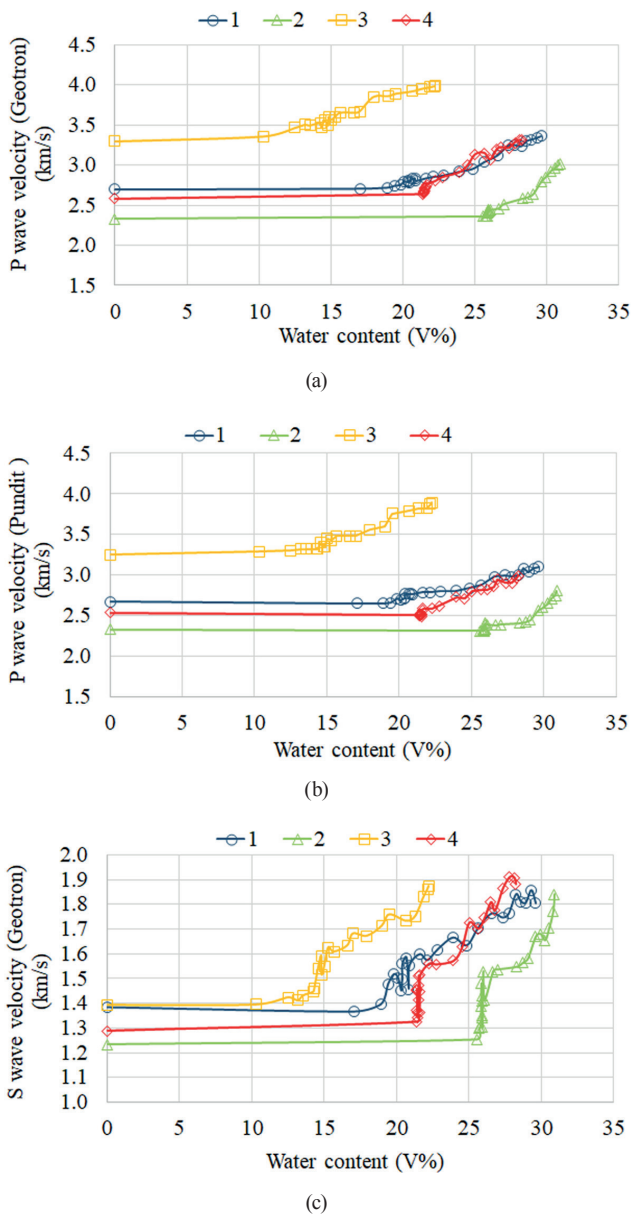
(a)

(b)

(c)

Fig. 5 The results of water saturation test a) P wave velocity (Geotron) vs. water content (V%), b) P wave velocity (Pundit) vs. water content (V%), c) S wave velocity (Geotron) vs. water content (V%)

velocity changed as the water content increased. The ultrasonic velocities of the stone were highly influenced by its water content and density (composition).

Generally, with rising water content, P wave velocity increased for all the samples. Initially, with increasing water content, the P wave velocities were almost constant for all the samples. As the stones reached their saturation phase, the P wave velocity rose moderately. This rising trend continued until all the samples were fully saturated.

After complete saturation, P wave velocity increased 24.67%, 29.75%, 20.86% and 28.29% for samples 1, 2, 3 and 4, respectively. The highest increase of P wave velocity

was found in samples 2 and 4. The trends of P wave velocities versus water content (V%) based on Pundit measurement is presented in Fig. 5(b).

At the end of the saturation process, the P wave velocities with the Geotron measurement were 8.5% higher than those measured with Pundit equipment. The trend of S wave velocities versus water content (V%) are demonstrated in Fig. 5(c). For all the samples, initially with increasing water percentage, the S wave velocities were almost constant. Then, the S wave velocities started to increase moderately as the percentage of water increased and this upward trend continued until the samples reached a complete saturation. After the saturation process was completed, S wave velocities increased 34.25%, 48.71%, 35.55% and 48.32% for sample 1, 2, 3 and 4, respectively. Sample 2 and 4 had the maximum increase of S wave velocity.

The percentage of weight change after the salt crystallization cycles was used to estimate decay. The results were plotted in Fig. 6 and Fig. 7 that showed the weight changes of samples after salt crystallization cycles with sodium sulphate and sodium chloride solutions versus the number of cycles, respectively. According to Fig. 6, there was an increasing trend in the weight of samples before the 4th
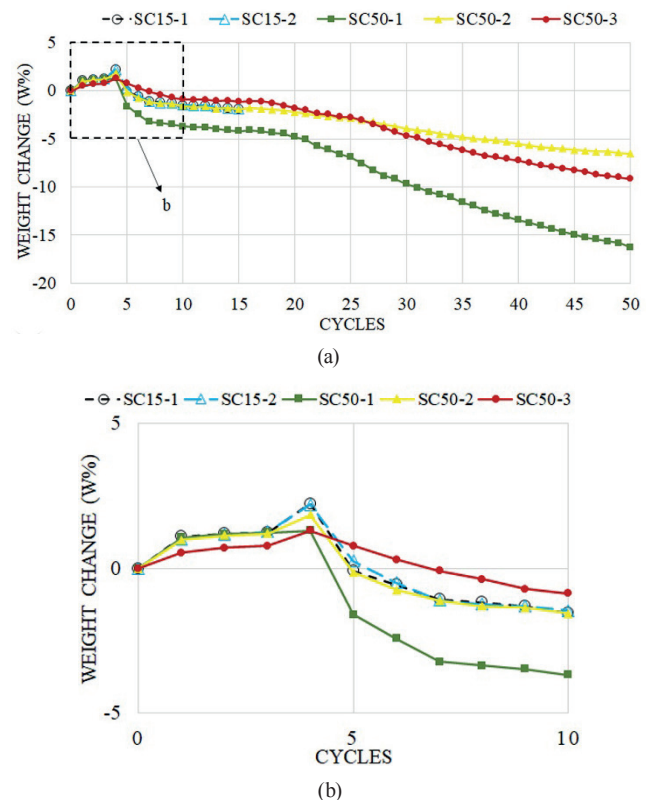

(a)

(b)

Fig. 6 Weight changes of samples after sodium sulphate crystallisation cycles a) 50 cycles and b) enlarged graph up to 10 salt crystallisation cycles sample codes are presented in Table 1)
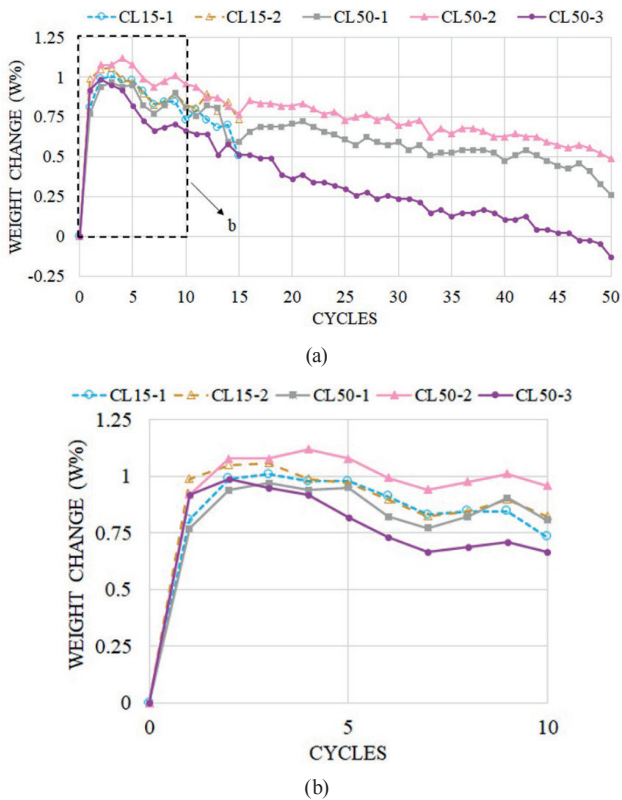
(a)

(b)

Fig. 7 Weight changes of samples after sodium chloride crystallization cycles a) 50 cycles, b) enlarged graph up to 10 salt crystallization cycles sample codes are presented in Table 1)

cycle of salt crystallization. Following that, the trend was reversed, and the weight of samples was decreased rapidly until 7th salt crystallization cycle. Then, the weight of samples was decreased slightly between 7th and 18th salt cycle. Finally, the weight change of samples had a decrease trend moderately up to the end of salt crystallization cycles. Sample SC50-1 had the highest amount of weight loss equal to 16 w% and sample SC50-2 had the lowest amount of weight loss equal to 6 w%

Fig. 7 shows an increase in the weight of samples up to 2 salt crystallization cycles with sodium chloride. Then, the weight of the samples was almost constant up to cycle 5. After that, the weight of samples had a decreasing trend until 50 salt cycles. However, the weight loss was insufficient to reduce the samples' weight in comparison to their initial weight, except for sample CL50-3, which had 0.13% weight loss compared to before salt crystallization.

The samples were microscopically examined after each salt crystallization cycle. The treatment with sodium sulphate and sodium chloride solutions exhibited two different levels of weathering. Both of them caused damage on the samples, but the effect of sodium sulphate was much greater than another salt.

In the case of sodium sulphate crystallization test, all the samples experienced different types of weathering including salt efflorescence, granular disintegration, cavities and pore enlargement. The granular disintegration of the samples continued steadily as the number of salt cycles increased until 50 salt cycles. Micro and macro cracks and erosion of the edge were observed on the sample SC50-3 (Fig. 8). This had cracks before starting salt crystallization process (Fig. 8(a)).

The cracks gradually expanded to the edges of the specimen (Fig 8(b) and Fig 8(c)) and ended up with creating cavities and erosions in the edge of the sample after 50 salt cycles (Fig. 8(d)) and the thickness of the cracks also expanded to 1.5 mm after 50 salt cycles (Fig. 8(d)). The heterogeneity of the sample SC50-3 increased after 50 salt cycles because of the fracturing and crack propagation in several directions.

During the sodium chloride crystallization tests salt efflorescence was formed on all the samples, but significant macroscopic signs of damage and crack propagation were not observed. The level of damage on the structure was lower than samples treated with another salt. Sodium chloride did not have a significant effect on the form of samples after salt crystallization cycles.

P wave velocity change based on the velocity of the non-weathered stone (%) show an increase before 15 salt crystallization cycles (Fig. 9) due to the deposition of salts in the pores. Then the trend was reversed, and P wave velocities gradually decreased until 50 salt cycles.

The trend of the curves was almost the same for all the samples up to 50 salt cycles. The highest increase for P wave velocity was around 15% (sample SC15-1) and
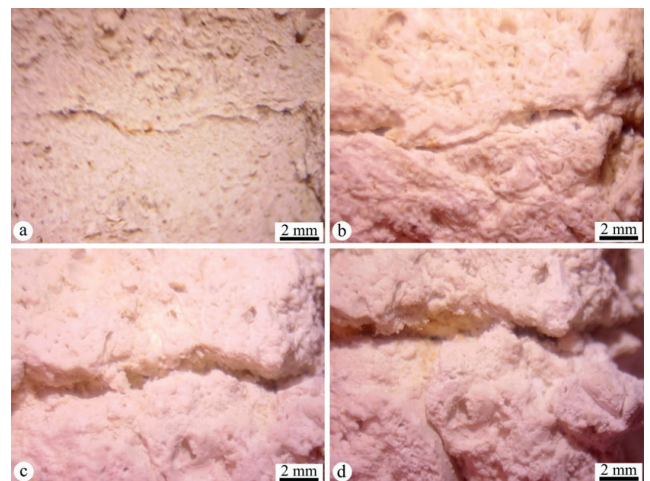

Fig. 8 Microscope images of sample SC50-3 a) before salt crystallization, b) after 15 salt cycles, c) after 30 salt cycles, d) after 50 salt cycles
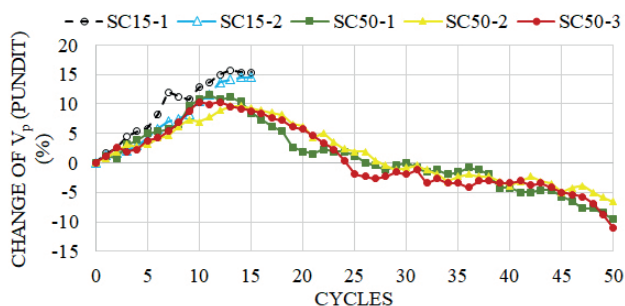
Fig. 9 P wave velocity changes after sodium sulphate crystallization test (sample codes are presented in Table 1)
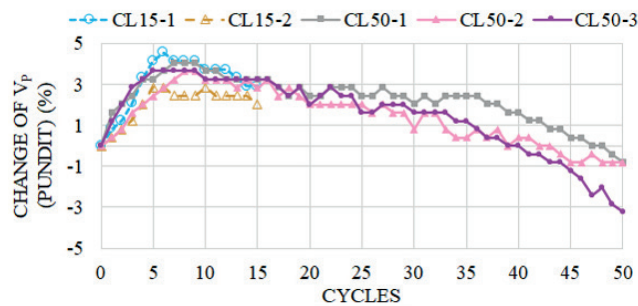

Fig. 10 P wave velocity changes after sodium chloride crystallization test (sample codes are presented in Table 1)

the highest amount of decrease for P wave velocity was around 12.5% (sample SC50-3). The lowest increase for P wave velocity before 15 salt cycle was 9.69% (sample SC50-2) and the lowest decrease for P wave velocity in cycle 50 was 6.5% percent (Sample SC50-2). A detailed look at Fig. 9 shows that the rate of P wave velocity loss after 50 salt cycles in the sample SC50-3 was greater than its initial rate of increase before 15 salt cycles and vice versa was true for other samples.

The results of P wave velocity changes (%) versus the number of salt cycles for samples treated with sodium chloride are demonstrated in Fig. 10. The results revealed that P wave velocity had an increasing trend up to cycle 5. After that, the P wave velocities had a constant process and gradually decreased with a steady slope until the salt

cycles ended. The maximum P wave velocity increase was around 4.5% on cycle 6 (sample CL15-1), and the maximum P wave velocities loss was around 3.2 % on cycle 50 (sample CL50-3).

A detailed look at Fig. 10 revealed that all the samples reached their maximum P wave velocities between cycle 5 and cycle 10. By comparing the initial increase of P wave velocity before cycle 8 and its final decrease in cycle 50, sample CL50-3 had the highest rate of P wave velocity changes.

A comparison between the results of Pundit and Geotron devices for all samples including non-weathered samples and samples after salt crystallization cycles with sodium sulphate and sodium chloride solutions are provided in Table 2. All the numbers in the table were the average of five repetitions, and the reported average results were

Table 2 P and S wave velocities of samples with the standard deviations (std)

Salt solution	Sample code	Salt crystallization cycle	P wave velocity (km/s)		S wave velocity (km/s)
			Pundit (Std. dev)	Geotron (Std. dev)	Filter (±3000 Hz) (Std. dev)
	3	-	3.25 (0.04)	3.30 (0.10)	1.39 (0.09)
Without salt crystallization (Group A)	1	-	2.68 (0.06)	2.70 (0.06)	1.38 (0.07)
	2	-	2.33 (0.06)	2.33 (0.04)	1.23 (0.06)
	4	-	2.54 (0.06)	2.58 (0.05)	1.29 (0.11)
	Average	-	2.52 (0.06)	2.54 (0.05)	1.30 (0.08)
14 w% Na2SO4·10H2O (Group B)	SC15-1	15	2.80 (0.07)	2.84 (0.09)	1.37 (0.35)
	SC15-2	15	2.76 (0.04)	2.88 (0.08)	1.51 (0.22)
	Average	-	2.78 (0.06)	2.86 (0.09)	1.44 (0.29)
	SC50-1	50	2.34 (0.04)	2.27 (0.13)	1.37 (0.23)
	SC50-2	50	2.41 (0.05)	2.46 (0.14)	1.48 (0.16)
	SC50-3	50	2.33 (0.03)	2.34 (0.07)	1.51 (0.06)
	Average	-	2.36 (0.04)	2.36 (0.11)	1.45 (0.15)
5 w% NaCl (Group C)	CL15-1	15	2.49 (0.02)	2.55 (0.05)	1.40 (0.21)
	CL15-2	15	2.51 (0.03)	2.57 (0.06)	1.37 (0.14)
	Average	-	2.50 (0.03)	2.56 (0.06)	1.39 (0.18)
	CL50-1	50	2.44 (0.03)	2.51 (0.08)	1.41 (0.11)
	CL50-2	50	2.47 (0.03)	2.56 (0.07)	1.44 (0.07)
	CL50-3	50	2.39 (0.04)	2.47 (0.07)	1.46 (0.10)
	Average	-	2.43 (0.03)	2.51 (0.07)	1.44 (0.09)

calculated based on the numbers in the table. Sample 3 had a higher density than the other samples, so it was not considered to calculate the average for non-weathered samples.

Based on Table 2, both sodium sulphate and sodium chloride solutions had an increasing effect on the P wave velocities of samples after 15 cycles of salt crystallization. Effect of sodium sulphate was greater than that of sodium chloride, because samples treated with sodium sulphate experienced more weight increase during the initial salt cycles than samples treated with another salt. As a consequence of weight increase, salts were deposited in the pores, the porosity of samples decreased and the density increased.

Sodium sulphate solution had a decreasing effect on the P wave velocities of samples after 50 salt cycles, however, the P wave velocities of samples did not change significantly after 50 salt cycle with sodium chloride solution. The average of P wave velocities by Geotron measurement for samples without salt crystallization, samples after 50 salt cycles with sodium sulphate and sodium chloride solutions were 2.52, 2.36, and 2.51 km/s, respectively. The minimum amount of P wave velocity belonged to the samples treated with sodium sulphate, because they had a more weight loss than samples submerged in another salt after 50 cycles. The same result can be concluded for the results of the Pundit device. Consequently, cavities and cracks in the samples reduced the P wave velocities of samples treated with sodium sulphate.

Shear wave velocities of samples changed significantly after salt crystallization test with both salt solutions. S wave velocity had an increasing trend from non-weathered samples to 50 salt cycles, and its trend was almost the same for samples treated with both salt solutions. The samples treated with sodium sulphate solution had a higher average S wave velocity than the samples treated with another salt after 15 and 50 salt cycles.

The trends of P and S waves velocities were different for samples subjected to salt crystallization. The standard deviation was increasing for the results of Geotron equipment after salt cycles and vice versa was true for the results of Pundit. The reason for this difference was that in the Pundit equipment, plasticine was used to cover the space between the sample and the transducer. While plasticine was not used in the Geotron equipment and increasing erosion of the edges and surface heterogeneity of the samples enhanced the discrepancies in the results.

A higher standard deviation was obtained for the results of the samples treated with sodium sulphate solution rather than another salt solution. The higher variability of the standard deviation can be understood by considering the micro-textural and micro-structural heterogeneity of samples. A comparison between the results of P wave velocity showed that the discrepancy between Pundit and Geotron measurements was less than 5 percent.

3 Discussion

The capillary water uptake tests showed that the highest amounts of capillary water uptake coefficient belonged to the samples with lower density and higher porosity which was consistent with the results of Ozcelik and Ozsguven [27]. In the present study, with rising water content the P wave velocity of rock increased. At first P wave velocity increased slowly and after the samples reached the saturation phase, their P wave velocities increased rapidly. Based on Çelik [8], capillary water absorption was high in rocks with a lot of capillary pores, which implied they can absorb water quickly by capillary uptake [8].

According to Benavente et al. [28], the highest capillary water absorption values were found in porous rocks with large pores (pore-throat size higher than 1 mm) and high porosity values ($\phi > 10\%$) which was consistent with the result of the present study. In the present study, the porosity of samples was higher than 10% and the size of macro pores were between 1 mm and 9 mm. The capillary water absorption was calculated in two ways based on [6] and EN 1925 [24]. Based on the first way after [6], all the samples had high capillary water absorption at the end of saturation (higher than 6.18 kg/m^2. s$^{0.5}$) and sample 2 had the highest porosity values (30.89 V%) and the highest water capillary absorption (9.64 kg/m^2. s$^{0.5}$). Also, the results of this study were consistent with the results of Barbera et al. [9] for capillary water absorption tests. According to Barbera et al. [9] the highest capillary absorption coefficient belonged to the most porous samples. In the present study, based on the second way (EN 1925 [24]), the highest capillary water absorption coefficient was 1.065 kg/m^2.s$^{0.5}$ and it was belonging to the sample 2 which had the highest porosity value (30.89 V%).

The results showed that the values of the P and S waves velocities changed as the water content increased. At first, the P and S waves velocities increased slowly. However, they rose at a faster rate as the saturation phase started. In samples with a lower density, the S wave velocity increased significantly. In water saturation test, the discrepancy between the results of Pundit and Geotron were around 8.5%, on average. As overall assessment, this study demonstrated that the P and S waves velocities were a function

of water content, and the changing in this parameter had an important effect on ultrasonic pulse velocities of limestone. With rising humidity, the P and S wave velocities increased more in the samples with lower density and higher porosity. Comparing the results of P and S waves velocities shows that the rate of increase in S wave velocity was higher than the P wave velocity increase. The results of this study were in agreement with the results of previous studies [8, 29, 30, 31, 32, 33]. Çelik [8] found an increasing trend for longitudinal wave velocity of natural stones after water saturation and freeze-thaw cycles. According to Karakul and Ulusay [29], ultrasonic velocity is controlled by porosity and humidity. P wave velocity was lower in stones with higher porosity and enhanced as the water content rose. In another research, an increase for P wave velocity of travertines was observed after water saturation [30]. Vasconcelos et al. [31] concluded that for granite and basalt, moisture content had a considerable influence on UPV, and UPV rose with increasing moisture content. Zhuang et al. [32] found that P and S wave velocities of granite rose by 27% and 13% in a water-saturated state. Li et al. [33] observed an increasing trend for the S wave velocity of porous sandstone after water saturation.

In the salt crystallization tests, salts crystallize in the pores and affect them in different ways. The form of samples changed significantly after sodium sulphate crystallization test. This change became more significant after 50 salt cycles. Weathering was observed in the form of granular disintegration, cavity, pore enlargement and crack. The differences in the rate of damages were due to the pre-existing cracks and cavities of the samples. However, the samples were not seriously affected by the sodium chloride crystallization test and the effect of sodium sulphate was found to be more destructive than another salt. According to Beck and Al-Mukhtar [34] NaCl did not cause significant damage in immersion tests. Under continuous capillarity solution supply, Rodriguez-Navarro and Doehne [10] evaluated the effects of NaCl and Na_2SO_4 on the weathering of oolitic limestone at two RH values. In these tests, NaCl was also less aggressive than Na_2SO_4. Because Na_2SO_4 easily creates supersaturated solutions, which is a stress-inducing mechanism [35, 36].

The petrophysical properties of the stones played a significant role in evaluating their susceptibility to salt damage. Former studies [1, 2, 10, 21] found that the amount of damage caused by salt crystallization in the stones was related to the amount of micropores and porosity. Stones with a high number of micropores and a large amount of porosity were more vulnerable to salt crystallization effect. Scherer [37] found that in materials with small pores, crystallization pressure was higher. After immersing porous limestone in a sodium sulphate solution and drying it at high temperatures, anhydrous Na_2SO_4 (thenardite) was formed in the present study. After cooling and immersing in a Na_2SO_4 solution again, the subsequent crystallization of mirabilite produced enough stress to degrade the stone. Small pores in the studied limestone caused high supersaturation ratios of the sodium sulphate before crystallization. High supersaturation ratios caused high sodium sulphate crystallization pressure and finally caused significant damage to the porous rocks.

Both sodium sulphate and sodium chloride crystallization increased the weight and the P wave velocities of samples during the first salt cycles. Then they reduced the weight and P wave velocities of the samples due to their destructive effects on the structure of the samples until the end of salt cycles.

The effect of sodium sulphate solution on the weight change and P wave velocities of samples were much more than that of sodium chloride solution. In the previous studies [34, 38], stones after sodium chloride crystallization tests experienced lower weight loss rather than other stones after sodium sulphate crystallization tests. Also, P wave velocity of samples treated with sodium sulphate was reduced more than that of samples treated with sodium chloride [39]. In the present study, the weight loss trend after salt crystallization cycles is similar to the weight loss trend of Italian limestone [9, 40], Portuguese limestones [41] and Aragon (Spain) sedimentary rocks [2] after salt cycles.

The trend between the weight change and P wave velocities of samples treated with sodium sulphate solution was not parallel because the weight change was up to 4 cycles positive and P wave velocity increased up to 15 cycle. The damages of rocks in this study were not consistent with the results of Angeli et al [11]. According to Angeli et al. [11], the damage caused by salt crystallization was divided into three stages. In the present study, the process of salt crystallization occurred in two stages. At first, the weight of samples increased and after that it decreased rapidly until the end of salt cycles.

The trend of S wave velocities was increasing after salt cycles for samples treated with both salt solutions, because salts were not washed out in water after salt cycles.

5 Conclusions

P and S waves velocities of non-weathered samples were influenced by water content. With increasing the water content, the P and S waves velocities increased. For samples with lower density and higher porosity, the changes of P and S wave velocities were higher than the samples with higher density and lower porosity.

Sodium sulphate solution had a more destructive effect on the structure of samples after weathering rather than sodium chloride solution, samples treated with sodium sulphate had a higher rate of damage including granular disintegration, pitting, pore enlargement and cracks. It was also discovered that the more pre-existing cracks and pores in the rock, the more damage was sustained. The trend of weight changes was different for the two salts. Treatment with sodium sulphate solution caused much higher weight change than the treatment with sodium chloride.

The trend of P wave velocity change was not the same in the case of both salts. The average P wave velocity for samples treated with sodium sulphate was higher than that of samples treated with sodium chloride after 15 salt cycles. P wave velocity loss was much higher for samples treated with sodium sulphate after 50 salt cycles than for samples treated with another salt. The trend of S wave velocity was the same for both groups of samples and it was increasing up to 50 salt cycles.

Acknowledgement

References

[1] Çelik, M. Y., Sert, M. "An assessment of capillary water absorption changes related to the different salt solutions and their concentrations ratios in the Döğer tuff (Afyonkarahisar-Turkey) used as building stone of cultural heritages", Journal of Building Engineering, 35, Article number: 102102, 2021.
https://doi.org/10.1016/j.jobe.2020.102102

[2] Buj, O., Gisbert, J. "Influence of pore morphology on the durability of sedimentary building stones from Aragon (Spain) subjected to standard salt decay tests", Environmental Earth Sciences, 61(7), pp. 1327–1336, 2010.
https://doi.org/10.1007/s12665-010-0451-4

[3] Sawdy, A., Heritage, A., Pel, L. "A review of salt transport in porous media, assessment methods and salt reduction treatments", Salt Weathering on Buildings and Stone Sculptures, The National Museum Copenhagen, Copenhagen, Denmark, 2008.

[4] Karoglou, M., Moropoulou, A., Giakoumaki, A., Krokida, M. K. "Capillary rise kinetics of some building materials", Journal of Colloid and Interface Science, 284(1), pp. 260–264. 2005.
https://doi.org/10.1016/j.jcis.2004.09.065

[5] Tomašić, I., Lukić, D., Peček, N., Kršinić, A. "Dynamics of capillary water absorption in natural stone", Bulletin of Engineering Geology and the Environment, 70(4), pp. 673–680, 2011.
https://doi.org/10.1007/s10064-011-0355-x

[6] Çelik, M. Y., Kaçmaz, A. U. "The investigation of static and dynamic capillary by water absorption in porous building stones under normal and salty water conditions", Environmental Earth Sciences, 75(4), Article number: 307, 2016.
https://doi.org/10.1007/s12665-015-5132-x

[7] Sengun, N., Demirdag, S., Akbay, D., Ugur, I., Altindag, R., Akbulut, A. "Investigation of The Relationships Between Capillary Water Absorption Coefficients And Other Rock Properties of Some Natural Stones", In: V. Global Stone Congress, Antalya, Turkey, 2014, pp. 22–25.

[8] Çelik, M. Y. "Water absorption and P-wave velocity changes during freeze–thaw weathering process of crosscut travertine rocks", Environmental Earth Sciences, 76(12), Article number: 409, 2017.
https://doi.org/10.1007/s12665-017-6632-7

[9] Barbera, G., Barone, G., Mazzoleni, P., Scandurra, A. "Laboratory measurement of ultrasound velocity during accelerated aging tests: Implication for the determination of limestone durability", Construction and Building Materials, 36, pp. 977–983, 2012.
https://doi.org/10.1016/j.conbuildmat.2012.06.029

[10] Rodriguez-Navarro, C., Doehne, E. "Salt weathering: influence of evaporation rate, supersaturation and crystallization pattern ", Earth Surface Processes and Landforms: The Journal of the British Geomorphological Research Group, 24(3), pp. 191–209, 1999.
https://doi.org/10.1002/(SICI)1096-9837(199903)24:3<191::AID-ESP942>3.0.CO;2-G

[11] Angeli, M., Bigas, J.-P., Benavente, D., Menéndez, B., Hébert, R., David, C. "Salt crystallization in pores: quantification and estimation of damage", Environmental Geology, 52(2), pp. 205–213, 2007.
https://doi.org/10.1007/s00254-006-0474-z

[12] Hamdi, E., Lafhaj, Z. "Microcracking based rock classification using ultrasonic and porosity parameters and multivariate analysis methods", Engineering Geology, 167, pp. 27–36, 2013.
https://doi.org/10.1016/j.enggeo.2013.10.008

[13] Brotons, V., Tomás, R., Ivorra, S., Grediaga, A., Martínez-Martínez, J., Benavente, D., Gómez-Heras, M. "Improved correlation between the static and dynamic elastic modulus of different types of rocks", Materials and Structures, 49(8), pp. 3021–3037, 2016.
https://doi.org/10.1617/s11527-015-0702-7

[14] Benavente, D., Martinez-Martinez, J., Cueto, N., Ordóñez, S., Garcia-del-Cura, M. A. "Impact of salt and frost weathering on the physical and durability properties of travertines and carbonate tufas used as building material", Environmental Earth Sciences, 77(4), Article number: 147, 2018.
https://doi.org/10.1007/s12665-018-7339-0

[15] Wang, Q., Ji, S., Sun, S., Marcotte, D. "Correlations between compressional and shear wave velocities and corresponding Poisson's ratios for some common rocks and sulfide ores", Tectonophysics, 469(1–4), pp. 61–72, 2009.
https://doi.org/10.1016/j.tecto.2009.01.025

[16] Uyanık, O., Sabbağ, N., Uyanık, N. A., Öncü, Z. "Prediction of mechanical and physical properties of some sedimentary rocks from ultrasonic velocities", Bulletin of Engineering Geology and the Environment, 78(8), pp. 6003–6016, 2019.
https://doi.org/10.1007/s10064-019-01501-6

[17] CEN "EN 12370 Natural stone test methods-determination of resistance to salt crystallization", European Committee for Standardization, Brusseles, Belgium, 1999.

[18] Török, Á. "Oolitic limestone in a polluted atmospheric environment in Budapest: weathering phenomena and alterations in physical properties", Geological Society, London, Special Publications, 205(1), pp. 363–379, 2002.
https://doi.org/10.1144/GSL.SP.2002.205.01.26

[19] Török, Á., Müller, C., Hüpers, A., Hoppert, M., Siegesmund, S., Weiss, T. "Differences in texture, physical properties and microbiology of weathering crust and host rock: a case study of the porous limestone of Budapest (Hungary)", In: Prykril, R., Smith, J. B. (eds.) Building Stone Decay: From Diagnosis to Conservation, Geological Society, London, UK, 2007, pp. 261–276.
https://doi.org/10.1144/GSL.SP.2007.271.01.25

[20] Pápay, Z., Rozgonyi-Boissinot, N., Török, Á. "Freeze–Thaw and Salt Crystallization Durability of Silica Acid Ester Consolidated Porous Limestone from Hungary", Minerals, 11(8), Article number: 824, 2021.
https://doi.org/10.3390/min11080824

[21] Belfiore, C. M., Calabrò, C., Ruffolo, S. A., Ricca, M., Török, Á., Pezzino, A., La Russa, M. F. "The susceptibility to degradation of stone materials used in the built heritage of the Ortygia island (Syracuse, Italy): A laboratory study", International Journal of Rock Mechanics and Mining Sciences, 146, Article number: 104877, 2021.
https://doi.org/10.1016/j.ijrmms.2021.104877

[22] Selwitz, C., Doehne, E., "The evaluation of crystallisation modifiers for controlling salt damage to limestone", Journal of Cultural Heritage, 3(3), pp. 205–216, 2002.
https://doi.org/10.1016/S1296-2074(02)01182-2

[23] Eyssautier-Chuine, S., Marin, B., Thomachot-Schneider, C., Fronteau, G., Schneider, A., Gibeaux, S., Vazquez, P. "Simulation of acid rain weathering effect on natural and artificial carbonate stones", Environmental Earth Sciences, 75(9), Article number: 748, 2016.
https://doi.org/10.1007/s12665-016-5555-z

[24] CEN EN 1925 Natural stone test methods- determination of water absorption coefficient by capillarity", European Committee for Standardization, Brusseles, Belgium, 1999.

[25] CEN "EN 13755 Natural stone test methods-determination of water absorption at atmospheric pressure", European Committee for Standardization, Brusseles, Belgium, 2002.

[26] Rozgonyi-Boissinot, N., Khodabandeh, M. A., Besharatinezhad, Á., Török, A. "Salt weathering and ultrasonic pulse velocity: condition assessment of salt damaged porous limestone", In: IOP Conference Series: Earth and Environmental Science, 833, Turin, Italy, 2021, Article number: 012070.
https://doi.org/10.1088/1755-1315/833/1/012070

[27] Ozcelik, Y., Ozguven, A. "Water absorption and drying features of different natural building stones", Construction and Building Materials, 63, pp. 257–270, 2014.
https://doi.org/10.1016/j.conbuildmat.2014.04.030

[28] Benavente, D., Pla, C., Cueto, N., Galvañ, S., Martínez-Martínez, J., García-del-Cura, M. A. Ordóñez, S. "Predicting water permeability in sedimentary rocks from capillary imbibition and pore structure", Engineering Geology, 195, pp. 301–311, 2015.
https://doi.org/10.1016/j.enggeo.2015.06.003

[29] Karakul, H., Ulusay, R. "Empirical correlations for predicting strength properties of rocks from P-wave velocity under different degrees of saturation", Rock Mechanics and Rock Engineering, 46(5), pp. 981–999, 2013.
https://doi.org/10.1007/s00603-012-0353-8

[30] Török, Á., Vásárhelyi, B. "The influence of fabric and water content on selected rock mechanical parameters of travertine, examples from Hungary", Engineering Geology, 115, pp. 237–245, 2010.
https://doi.org/10.1016/j.enggeo.2010.01.005

[31] Vasconcelos, G., Lourenço, P. B., Alves, C. A. S., Pamplona, J. "Ultrasonic evaluation of the physical and mechanical properties of granites", Ultrasonics, 48(5), pp. 453–466, 2008.
https://doi.org/10.1016/j.ultras.2008.03.008

[32] Zhuang, L., Kim, K. Y., Diaz, M., Yeom, S., "Evaluation of water saturation effect on mechanical properties and hydraulic fracturing behavior of granite", International Journal of Rock Mechanics and Mining Sciences, 130, Article number: 104321, 2020.
https://doi.org/10.1016/j.ijrmms.2020.104321

[33] Li, D., Wei, J., Di, B., Ding, P., Huang, S., Shuai, D. "Experimental study and theoretical interpretation of saturation effect on ultrasonic velocity in tight sandstones under different pressure conditions", Geophysical Journal International, 212(3), pp. 2226–2237, 2018.
https://doi.org/10.1093/gji/ggx536

[34] Beck, K., Al-Mukhtar, M. "Evaluation of the compatibility of building limestones from salt crystallization experiments", Geological Society, London, Special Publications, 333(1), pp. 111–118, 2010.
https://doi.org/10.1144/SP333.11

[35] Steiger, M., Asmussen, S. "Crystallisation of sodium sulfate phases in porous materials: The phase diagram Na2SO4–H2O and the generation of stress", Geochimica et Cosmochimica Acta, 72(17), pp. 4291–4306, 2008.
https://doi.org/10.1016/j.gca.2008.05.053

[36] Ottosen, L. M. "Electro-desalination of sulfate contaminated carbonaceous sandstone–risk for salt induced decay during the process", In: Hughes, J. J., Howind, T. (eds.) Science and Art: A Future for Stone: Proceedings of the 13th International Congress on the Deterioration and Conservation of Stone, 2, 2016, pp. 897–904.

[37] Scherer, G. W. "Stress from crystallization of salt", Cement and Concrete Research, 34(9), pp. 1613–1624, 2004.
https://doi.org/10.1016/j.cemconres.2003.12.034

[38] Rothert, E., Eggers, T., Cassar, J., Ruedrich, J., Fitzner, B., Siegesmund, S. "Stone properties and weathering induced by salt crystallization of Maltese Globigerina Limestone", Geological Society, London, Special Publications, 271(1), pp. 189–198, 2007.
https://doi.org/10.1144/GSL.SP.2007.271.01.19

[39] Çelik, M. Y., İbrahimoglu, A. "Characterization of travertine stones from Turkey and assessment of their durability to salt crystallization", Journal of Building Engineering, 43, Article number: 102592, 2021.
https://doi.org/10.1016/j.jobe.2021.102592

[40] La Russa, M. F., Ruffolo, S. A., Belfiore, C. M., Aloise, P., Rovella, N., Randazzo, L., Pezzino, A., Montana, G. "Study of the effects of salt crystallisation on degradation of limestone rocks", Periodico di Mineralogia, (Special Issue) Mineralogical Applications on Environments, Archaeometry and Cultural Heritage, 82(1), 2013.
https://doi.org/10.2451/2013PM0007

[41] Alves, C., Figueiredo, C., Maurício, A., Braga, M. A. S., Aires-Barros, L. "Limestones under salt decay tests: assessment of pore network-dependent durability predictors", Environmental Earth Sciences, 63(7), pp. 1511–1527, 2011.
https://doi.org/10.1007/s12665-011-0915-1